シングルパルスフェムト秒レーザーを用いた非平衡脱離過程の研究

王健仲[A]、兼松泰男[A]、 邨次敦[C]、松田冬樹[D]、松田若菜[B]、河井洋輔[B]、豊田岐聡[A、B]

大阪大学大学院理学研究科物理学専攻[A]、 大阪大学大学院理学研究科附属フォアフロント研究センター[B]、インディペンデントスカラー[C]、京都大学物質－細胞統合システム拠点[D]

Study on Non-equilibrium Desorption Processes Using Single-pulse Femtosecond Laser

J. Z. Wang[A], Y. Kanematsu[A], A. Muratsugu[C], F. Matsuda[D], W. Matsuda[B], Y. Kawai[B], M. Toyoda[A, B]

Department of Physics, Graduate School of Science, The University of Osaka[A], Forefront Research Center, Graduate School of Science, The University of Osaka[B], Independent Scholar[C]

Institute for Integrated Cell-Material Sciences, Kyoto University[D]

In this study, we developed a pulse-resolved time-of-flight (TOF) ion-profile acquisition system to investigate single-pulse ion emission dynamics from 1-μm-thick CsI deposits under femtosecond (fs) laser irradiation (800 nm, 180–1500 fs, 400–800 nJ). The resulting TOF ion profiles were analyzed with a single-pulse method-of-moments (SP-MOM) procedure to extract the number of ions (ion yield), the mean ion kinetic energy, and an effective ion temperature for each laser shot, and these parameters were evaluated relative to the Maxwellian equilibrium reference line. Compared with longer pulses, 180 fs irradiation produces higher kinetic energies, and exhibits a larger deviation from the equilibrium line, indicating a more pronounced non-equilibrium response. Slightly above the CsI deposits ablation threshold, 180 fs additionally exhibits a distinct high ion yield distribution, whereas 660 fs and 1500 fs remain confined to low ion yield distribution. These pulse-resolved measurements, combined with SP-MOM, expose pulse-to-pulse ablation characteristics that are obscured by ensemble averaging and provide a quantitative basis to compare non-equilibrium ion emission across pulse durations.

Introduction：

The ultrashort irradiation period of a femtosecond (fs) laser makes laser–material interactions a strongly non-equilibrium process [1]. During the initial non-equilibrium stage within the first ~100 fs, fast electrons escape from the solid and pull out cold ions through electrostatic attraction, leading to electrostatic ablation driven by small-scale fields near the vacuum interface. Over the subsequent several picoseconds, electron–ion collisions transfer energy from the hot electrons to the ions; once the average ion energy exceeds the binding energy, surface atoms and ions are emitted even though their energy distribution remains far from a Maxwellian. On a timescale of tens of picoseconds, frequent ion–ion collisions finally establish a Maxwellian energy distribution, and ablation proceeds as thermal evaporation that can be described using thermodynamic relations [2].

Although various physical models, including molecular-dynamics, hydrodynamic, and first-principles simulations, have reproduced key aspects of ultrafast laser–matter dynamics and provided important mechanistic insight [3], direct experimental observation of single-pulse ablation dynamics remains insufficient. To address this gap, we developed a pulse-resolved time-of-flight (TOF) ion-profile acquisition system to investigate ion emission from 1-

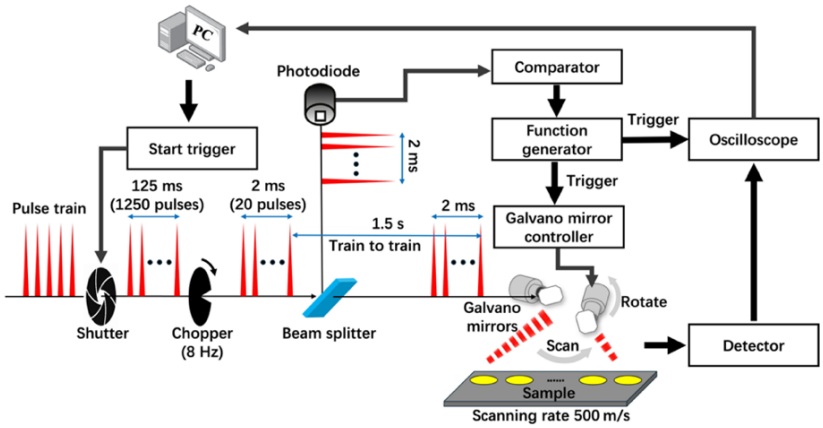

Fig.1. Block diagram of the single-pulse scanning-mode fs laser irradiation system.

μm-thick CsI deposits under fs laser irradiation (wavelength: 800 nm, pulse durations: 180–1500 fs; fluences: 130–260 mJ/cm^2).

In conventional TOF-profile-based ultrafast analysis, ion-velocity distributions are inferred by fitting models (e.g., shifted Maxwell–Boltzmann distributions) to ensemble-averaged TOF profiles accumulated over many laser pulses. Such averaging, however, conceals the single-pulse TOF behavior and pulse-to-pulse fluctuations in ion emission. In this work, we instead record TOF spectra on a single-pulse basis without averaging and apply a single-pulse method-of-moments (SP-MOM) analysis to extract, for each laser shot, the number of ions (ion yield) N, mean ion kinetic energy $\langle E \rangle$, and effective ion temperature σ_E. This approach enables the construction of statistical distributions that reveal pulse-resolved ablation dynamics inaccessible to ensemble-averaged analysis.

Experimental system development:

The schematic of the developed experimental setup involving TOF mass spectrometer and laser system has been described in our previous work [4]. Based on this setup, a newly developed measurement system was constructed. The block diagram is shown in Fig. 1. The measurement sequence begins with a start command that opens the shutter for 125 ms, allowing fs laser pulse trains to pass through. These continuous pulse trains are temporally modulated into 2 ms windows by a mechanical chopper, producing pulse bursts containing 20 pulses each at a 10 kHz repetition rate. The resulting pulse bursts are then split by a beam splitter. One portion of the beam is directed to the Galvano mirrors and focused onto the sample surface with a spot diameter of 20 μm. The other portion is sent to a photodiode, which converts the 800 nm laser pulses into an electrical voltage signal that is transmitted to a comparator. When the signal exceeds a predefined voltage threshold, the comparator generates a 2 ms TTL signal. This TTL signal simultaneously triggers both the function generator and the oscilloscope. Upon receiving the trigger, the function generator outputs a linearly increasing voltage to drive the Galvano mirror controller, which rotates the mirror and enabling lateral scanning synchronized with the pulse train. Consequently, the fs laser pulses are evenly distributed across the sample surface. At the same time, the triggered oscilloscope records the ion signals detected by a microchannel plate detector. All acquired signals are subsequently transferred to a computer for post-acquisition analysis.

Analysis method:

After acquiring the single-pulse ion TOF spectra, the ion initial kinetic energy $E = mv^2/2$ was calculated from the measured TOF using a one-

dimensional approximation:

$$TOF = \frac{-\sqrt{2E/m} + \sqrt{2(E+Uq)/m}}{Uq/mL_1} + \frac{L_2}{\sqrt{2(E+Uq)/m}}, \quad (1)$$

where the ion with mass-to-charge ratio (m/q) traverses through an acceleration region L_1 with acceleration voltage U and field-free region L_2. The TOF spectra were then converted to energy spectra with Eq. (1), and moments analysis was applied to each single-pulse ion energy spectrum. The 0th moment (spectral area) corresponds to the number of ions N detected in that event, the 1st moment gives the mean ion kinetic energy $\langle E \rangle$, and the 2nd moment (standard deviation of the spectrum) represents the ion-energy spread, which is used as an effective ion temperature σ_E. These procedures collectively constitute the SP-MOM analysis.

We also employed a one-dimensional, half-space Maxwellian velocity distribution $(v > 0)$ at temperature T for comparison,

$$f(v) = \sqrt{\frac{2m}{\pi k_B T}} \exp\left(-\frac{mv^2}{2k_B T}\right), \qquad v > 0. \quad (2)$$

Since E depends only on v^2, the truncation to $v > 0$ does not affect the even-order moments. Therefore, the 1st and 2nd moment of E are

$$\langle E \rangle = \frac{1}{2} k_B T, \qquad \sigma_E = \frac{k_B T}{\sqrt{2}}. \quad (3)$$

Consequently, a one-dimensional thermal equilibrium state satisfies the linear relation $\sigma_E / \langle E \rangle = \sqrt{2}$, and we use this line as a reference in the $\langle E \rangle$-σ_E plots.

Experimental results and discussion:

Fig. 2 summarizes the dependence of the single-pulse Cs^+ emission characteristics on laser intensity and pulse duration. Each CsI deposit was irradiated with 2000 fs laser shots, and a TOF spectrum of Cs^+ was recorded for every individual shot. Measurements were carried out at pulse energies of 400, 500, 700, and 800 nJ and pulse durations of 180, 660, and 1500 fs, and the TOF spectra containing detectable Cs^+ signals were analyzed using SP-MOM. In each panel, the σ_E is plotted against the $\langle E \rangle$ together with an equilibrium reference line defined by $\sigma_E / \langle E \rangle = \sqrt{2}$. At 400 nJ, ion emission events are observed only under 180 fs irradiation, whereas no detectable emission appears for longer pulse durations. Under this 400 nJ–180 fs condition, a small fraction of 180 fs events lies on the equilibrium line near $\langle E \rangle = 5$ eV, indicating

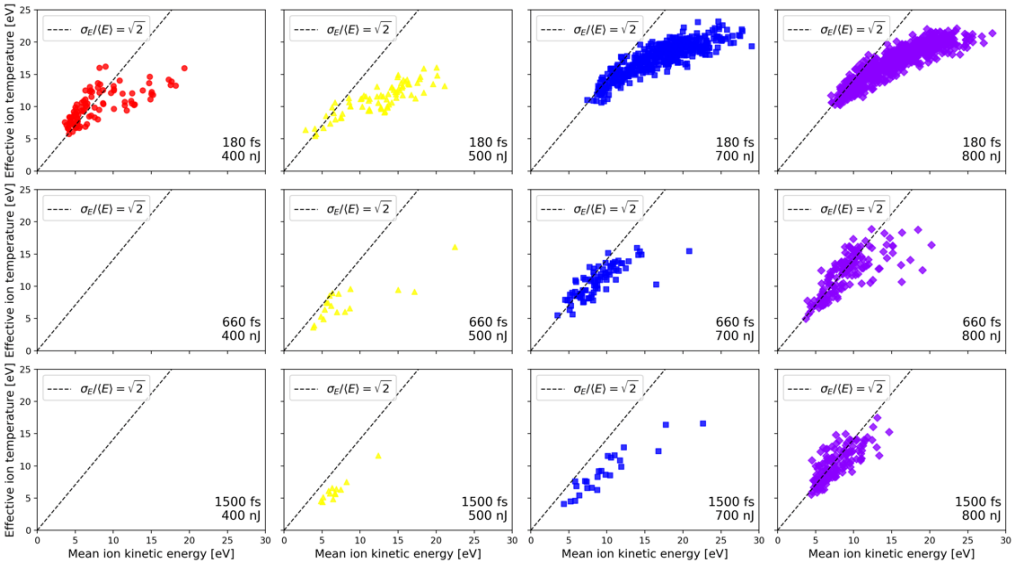

Fig. 2. Relationship between the mean ion kinetic energy and effective ion temperature.

emission consistent with or close to equilibrium, while another fraction shifts to the right of the line toward higher $\langle E \rangle$ at a given σ_E, indicating a non-equilibrium emission process. At 500 nJ, ion emission begins to appear for 660 fs and 1500 fs, and their distributions are closer to the equilibrium line than those for 180 fs case. As the pulse energy further increases (700–800 nJ), the 180 fs distributions shift toward higher $\langle E \rangle$ (7–30 eV) and σ_E (10–25 eV), moving progressively away from the equilibrium line. In contrast, the 660 fs and 1500 fs distributions remain concentrated near the equilibrium line over a moderately broad range of $\langle E \rangle$ (5–20 eV) and σ_E (5–20 eV), indicating that ion emission under longer pulses is closer to thermal equilibrium.

Because the ablation threshold fluence F_{th} for CsI deposits is ~250 mJ/cm² [5], the fluence at a pulse energy of 800 nJ (260 mJ/cm²) lies close to this threshold. Fig. 3 plots the N as a function of the $\langle E \rangle$ for different pulse durations at 800 nJ (the legend shows the corresponding peak intensities). Under the 180 fs condition, two distinct distributions are observed: a high ion yield distribution (dashed black box) with $\langle E \rangle$ (7–15 eV), and a low ion yield distribution (dashed green box) with $\langle E \rangle$ (13–27 eV). In contrast, the 660 fs and 1500 fs distributions confined to the low ion yield region, with lower $\langle E \rangle$ (4–14 eV).

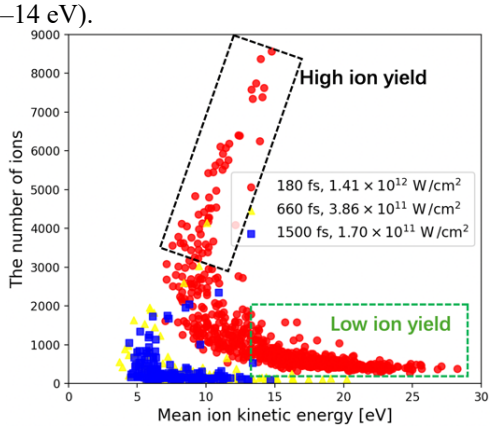

Fig. 3. The number of ions versus mean ion kinetic energy at 800 nJ for three pulse durations.

Electrostatic ablation is generally regarded as the dominant a-removal mechanism under non-equilibrium conditions near and slightly above the ablation threshold [2]. We therefore consider that the high $\langle E \rangle$, high ion yield distribution observed at 180 fs arises from additional ion acceleration driven by the transient electrostatic field. For the longer pulse durations, this field-driven contribution is substantially reduced, and enhanced electron–ion energy exchange promotes a quasi-thermal, near-equilibrium regime characterized by lower $\langle E \rangle$ and reduced ion yield.

Conclusion:

We developed a pulse-resolved TOF ion-profile acquisition system and applied a SP-MOM analysis to extract the ion yield, mean ion kinetic energy, and effective ion temperature for each laser shot. Interpreting these results against the Maxwellian equilibrium reference line $\sigma_E/\langle E \rangle = \sqrt{2}$, we found that 180 fs irradiation produces higher $\langle E \rangle$ and greater deviations from equilibrium than 660 fs and 1500 fs, indicating a stronger non-equilibrium response. Near and slightly above the CsI ablation threshold, 180 fs shows two distributions, while longer pulses remain in low ion yield, near-equilibrium regions. The high-energy distribution at 180 fs is likely driven by transient electrostatic-field acceleration, whereas longer pulses promote quasi-thermal behavior through enhanced electron–ion coupling. Overall, SP-MOM provides a pulse-resolved framework for quantifying non-equilibrium ablation dynamics beyond ensemble-averaged TOF analysis.

Reference

[1] L. Jiang *et.al.* Light Sci. Appl. 7 (2018) 17134.
[2] E. Gamaly et.al. Prog. Quantum Electron. 37 (2013) 215.
[3] L. V. Zhigilei et.al. Chem. Rev. 103 (2003) 321–348.
[4] J. Wang et.al. Results Phys. 76 (2025) 108415.
[5] M. Hada et.al. Nat. Commun. 5 (2014) 3863.